Optics Communications 413 (2018) 162–166

Contents lists available at ScienceDirect

Optics Communications

journal homepage: www.elsevier.com/locate/optcom

Enhancing the photon-extraction efficiency of site-controlled quantum dots by deterministically fabricated microlenses

Arsenty Kaganskiy, Sarah Fischbach, André Strittmatter [1], Sven Rodt, Tobias Heindel, Stephan Reitzenstein *

Institut für Festkörperphysik, Technische Universität Berlin, Hardenbergstraße 36, D-10623 Berlin, Germany

ARTICLE INFO

Keywords:
Site-controlled quantum dot
Single-photon source
In-situ electron-beam lithography
Microlens

ABSTRACT

We report on the realization of scalable single-photon sources (SPSs) based on single site-controlled quantum dots (SCQDs) and deterministically fabricated microlenses. The fabrication process comprises the buried-stressor growth technique complemented with low-temperature in-situ electron-beam lithography for the integration of SCQDs into microlens structures with high yield and high alignment accuracy. The microlens-approach leads to a broadband enhancement of the photon-extraction efficiency of up to (21 ± 2)% and a high suppression of multi-photon events with $g^{(2)}(\tau = 0) < 0.06$ without background subtraction. The demonstrated combination of site-controlled growth of QDs and in-situ electron-beam lithography is relevant for arrays of efficient SPSs which, can be applied in photonic quantum circuits and advanced quantum computation schemes.

1. Introduction

The development and optimization of quantum light sources is a central topic of quantum nanophotonics and quantum communication. The latter requires close to ideal properties in terms of suppression of multi-photon emission, photon indistinguishability, and entanglement fidelity to implement for instance the quantum repeater protocol for long-distance quantum communication [1]. In principle, self-assembled quantum dots (QDs) are supreme candidates to meet these stringent requirements. However, due to their random positions and emission energies it is a great technological challenge to integrate single QDs in a controlled manner into photonic structures to enhance their photon-extraction efficiency and to improve their quantum nature of emission. Popular approaches for efficient light outcoupling include photonic wires [2], micropillar cavities [3] and microlenses [4]. In parallel, during the last decade deterministic nanoprocessing technologies based on optical as well as electron-beam in-situ lithography have been developed and refined in order to integrate single self-assembled QDs into high-quality micropillar cavities [5], circular dielectric gratings [6] and microlenses [4]. Although this deterministic nanotechnology approach has been exploited very successfully for the realization of sources generating indistinguishable single-[7] or twin-[8] photon states based on self-organized QDs, it is less suitable for the realization of ordered arrays of quantum light sources, due to the random spatial position of the selected QDs. This represents a major hurdle for the realization of parallel optical links for, e.g., photonic quantum circuits that require a multitude of spectrally matched single-photon sources (SPSs). A prominent example is boson sampling on a photonic chip based on nonclassical interference of photons in an integrated photonic circuit, [9] and quantum computing based on photonic coupling in an array of QDs [10]. In order to upscale the realization of QD-based SPSs and to eventually enable such appealing applications, one needs to apply advanced growth techniques which allow for the site-controlled nucleation of single QDs. Prominent examples for the realization of site-controlled QDs are based on top-down etching techniques [11], site-selective growth on nanohole-arrays [12–14], inverted pyramids [15,16] and buried-stressors [17] respectively. In this work we present a concept which combines the advantages of site-controlled growth, in-situ electron-beam lithography (EBL) and microlenses to realize highly efficient single-photon emitters in a scalable nanotechnology platform.

We apply the buried stressor approach which is based on the selective oxidation of an AlAs add-layer in a semiconductor heterostructure [18]. The controlled oxidation allows for stress engineering in the overlying layers [19] due to a reduced volume of the oxidized layer by about 12–13% [20]. During a subsequent overgrowth, In(Ga)As QDs tend to

* Corresponding author.
E-mail address: stephan.reitzenstein@tu-berlin.de (S. Reitzenstein).

[1] Present address: Abteilung Halbleiterepitaxie, Otto-von-Guericke Universität Magdeburg, Universitätsplatz 2, D-39106 Magdeburg, Germany.

https://doi.org/10.1016/j.optcom.2017.12.032
Received 23 August 2017; Received in revised form 8 November 2017; Accepted 12 December 2017
0030-4018/

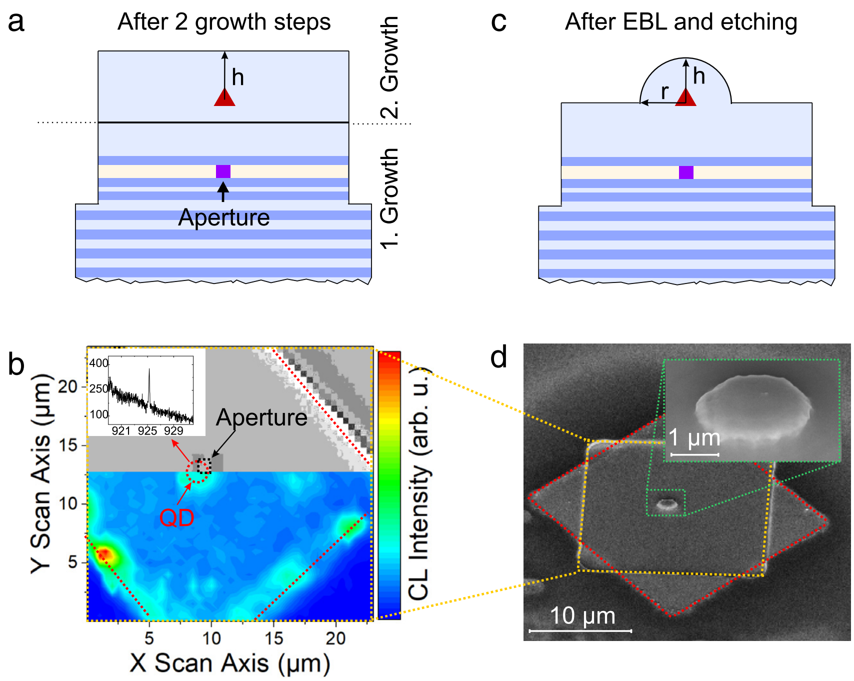

Fig. 1. Two excerpts of the work flow for fabricating SCQDs with deterministically placed microlenses: The two-step growth of the epitaxial structure via the buried stressor approach (a) is followed by microlens processing via in-situ EBL and subsequent ICP-RIE dry etching (c). (b) SEM image of a structure as shown in (a) with a recognizable aperture (top part) and 2D cathodoluminescence map of the same structure with the pronounced luminescence from the SCQD (bottom part) as described in the text (positions of the QD and the aperture are marked with a dashed circle and square, respectively). The spectrum of the corresponding QD taken during the in-situ EBL process is shown in the inset. (d) SEM image of a fully processed microlens structure (cf. inset). The mesa whose cross-section is sketched in (a) and (c) and the CL mapping area are marked in (b) and (d) with a dashed red and yellow rectangle, respectively. (For interpretation of the references to color in this figure legend, the reader is referred to the web version of this article.)

nucleate at the maximum tensile strain emerging over the underlying AlAs aperture. Hereby, the diameter of the aperture influences the strain distribution at the surface in a way that for small aperture diameters and proper adjusted QD growth parameters single QDs can be grown above the oxide aperture. Compared to QDs aligned to etched nanohole-arrays, this type of site-controlled QDs (SCQDs) does not suffer from close-by etched surfaces, enabling a high optical quality similar to that of standard self-assembled QDs [21]. This advantage is obtained at the cost of a rather gentle site-control which can lead to a slight displacement from the aperture's center towards the aperture's boundaries between the oxidized and non-oxidized regions. Therefore, the precise determination of the SCQD's position is inevitable before fabricating a microlens since a lateral displacement $\geq$ 50 nm of the emitter would lead to a significant decrease of the extraction efficiency [4]. In-situ EBL allows for an alignment accuracy of 34 nm [22] and, hence, fulfills the aforementioned requirements.

2. Sample fabrication and simulations

The sample fabrication is schematically presented in Fig. 1(a) and (c). It starts with the growth of the Al(Ga)As heterostructure via metalorganic chemical vapor deposition (MOCVD) on an n-doped GaAs (100) substrate based on the numerically optimized layer design (details on the simulation are given below). First, a 300 nm thick GaAs buffer layer and the DBR consisting of 27 pairs of $\lambda/4$ thick $Al_{0.90}Ga_{0.10}As$/GaAs are grown followed by a 30 nm thick AlAs layer sandwiched in 40 nm thick $Al_{0.90}Ga_{0.10}As$ claddings. The first growth step is finalized by an 80 nm thick GaAs capping layer. Next, an array of quadratic mesa structures with a base width of 20–21 µm is processed with a pitch of 260 µm into the template by UV lithography and inductively-coupled plasma reactive-ion dry etching (ICP-RIE). After selective oxidation of the apertures the second epitaxial growth step is performed. It starts with the growth of a 50 nm thick GaAs layer followed by the Stranski–Krastanow growth of InAs SCQDs and a 418 nm thick GaAs capping layer which corresponds to the numerically optimized height of the lenses (cf. Fig. 1(a)). Subsequently, the sample is spin-coated with 110 nm of the electron-beam resist CSAR 62 [23] followed by in-situ EBL [4,24]. The bottom part of Fig. 1(b) shows exemplarily a 2D cathodoluminescence (CL) map of the mesa surface taken during the CL lithography step. The map refers to the spectral range of 925.21–925.49 nm and indicates the pronounced luminescence of a charged trion state of the SCQD whose spectrum is shown in the inset. The position of this SCQD is marked by a dashed red circle in Fig. 1(b). At the edges of the overgrown mesa emission spots of defect centers are visible. Simultaneously, a scanning electron microscope (SEM) image is recorded (top part of the figure) demonstrating the aperture which can be identified due to a surface modulation caused by the modified strain in the underlying layers. Comparing both maps, moderate misalignment between the center of the aperture and the SCQD of about 800 nm is visible. During in-situ EBL, lenses with the optimized height (h = 418 nm) and radius (r = 1040 nm) (cf. Fig. 2 (a)) are written into the resist at the positions of the identified SCQDs. The CL mapping is performed with an exposure dose corresponding to the positive-tone regime of the used resist while the lens writing is done in the negative-tone regime [23]. This results resulting in a removal of the resist from the scanned area except for the lens position in the following development step (the mapped area is marked by a yellow dashed rectangle in Fig. 1(b) and (d)). The fabrication is finalized by ICP-RIE (cf. Fig. 1(c)) followed by an SEM-based analysis of the lateral displacement of the microlenses with respect to the aperture's centers. Fig. 1(d) presents an SEM image of the fully processed device and a zoom-in of the microlens (inset). It is noteworthy, that the presented approach provides a high yield for the realization of SCQDs. In the present study 17 out of 27 mesa structures contained a SCQD corresponding to a yield of 63%. The average displacement of the SCQDs from the center of the oxidized aperture was determined to be 640 nm for a given aperture side-length in the range between 1200 and 1600 nm.

Prior to the above-described sample fabrication, the structural design was optimized in order to maximize the photon-extraction efficiency η. The simulation results presented in Fig. 2 were obtained using the